Scientific Research Publishing

Open Journal of Fluid Dynamics, 2025, 15(3), 136-157
https://www.scirp.org/journal/ojfd
ISSN Online: 2165-3860
ISSN Print: 2165-3852

# Numerical Study of Heat Transfer in a Nanofluid-Filled Trapezoidal Enclosure with Star-Shaped Heat Sources under Magnetic Field

**Sree Pradip Kumer Sarker*, Md. Mahmud Alam**

Department of Mathematics, Dhaka University of Engineering and Technology (DUET), Gazipur, Bangladesh
Email: *pradip.duet@gmail.com, alamdr.mahmud@duet.ac.bd

**How to cite this paper:** Sarker, S.P.K. and Alam, Md.M. (2025) Numerical Study of Heat Transfer in a Nanofluid-Filled Trapezoidal Enclosure with Star-Shaped Heat Sources under Magnetic Field. *Open Journal of Fluid Dynamics*, **15**, 136-157.
https://doi.org/10.4236/ojfd.2025.153009

**Received:** May 28, 2025
**Accepted:** July 18, 2025
**Published:** July 21, 2025



## Abstract

Effective thermal management in geometrically irregular enclosures is crucial for optimizing performance in electronics cooling, renewable energy, and thermal engineering systems. This numerical study investigates conjugate magnetohydrodynamic (MHD) free convection heat transfer in a Cu-$H_2O$ nanofluid-filled trapezoidal cavity with a wavy (corrugated) top boundary and embedded internally heat-generating star-shaped copper obstacles. The cavity base angle(γ) is fixed at 15˚, and the simulation employs the Galerkin finite element method to solve coupled solid-fluid heat transfer equations under varying Rayleigh numbers ($Ra = 10^3$ - $10^6$), Hartmann numbers ($Ha$ = 15, 50), and nanoparticle volume fractions ($\phi$ = 0.01 - 0.03). The Galerkin finite element method (FEM) is employed due to its robustness in handling irregular geometries and complex boundary conditions. This method ensures accurate resolution of coupled thermal and fluid fields within the wavy trapezoidal cavity and around embedded star-shaped heat sources. Results reveal that both the shape and placement of star-shaped heaters strongly influence heat flow, enhancing convective mixing and thermal dispersion through vortex structures. The corrugated top wall further improves vertical heat transport. Increasing the nanoparticle concentration from 0.01 to 0.03 led to a significant enhancement in average Nusselt number and a reduction in average fluid temperature, demonstrating the superior heat transfer capability of nanofluids. At higher Rayleigh numbers, the dominance of buoyancy-induced flow over magnetic damping further amplified convective efficiency. The findings underscore the potential of integrating nanofluid technologies with complex geometry and internal heating to optimize thermal control in passive cooling applications and high-efficiency heat exchangers.

**Keywords**

Nanofluid, Trapezoidal Cavity, Magnetohydrodynamics, Natural Convection, Thermal Conductivity

## 1. Introduction

The optimization of heat transfer in enclosures with complex geometries using nanofluids and magnetohydrodynamic (MHD) effects has attracted extensive research interest due to its broad applications in thermal energy systems, electronic cooling, and advanced heat exchangers. Trapezoidal cavities, owing to their structural flexibility, have become a popular geometry in recent thermal studies, particularly when subjected to natural or mixed convection using various working fluids [1]-[4]. Nanofluids, such as Cu-water and hybrid formulations, offer enhanced thermal conductivity and flow characteristics that support more efficient convective mechanisms [5]-[8]. Investigations combining MHD effects and nanofluid convection in trapezoidal or wavy enclosures reveal that magnetic fields significantly influence boundary layer thickness, flow circulation, and heat transfer uniformity [9]-[13]. The incorporation of non-standard geometries—like corrugated, sinusoidal, and wavy boundaries—further modifies thermal gradients and promotes stronger vortex formations, especially in cases involving inclined or undulated walls [14]-[19]. Recent studies have also examined internal features such as heated cylinders, triangular blocks, and solid obstacles to understand conjugate heat transfer behavior and localized fluid motion [20]-[24]. Hybrid nanofluids with phase-change materials or metallic nanoparticles in porous and double-diffusive environments have shown marked improvements in thermal efficiency under both steady and oscillating magnetic fields [25]-[28]. Simulations using finite element and finite volume methods have demonstrated strong agreement with experimental results in capturing complex thermal-fluid interactions inside cavities with internal heat generation and varying thermal boundary conditions [29]-[33]. Star-shaped internal heaters are an emerging focus due to their geometric complexity, increased surface area, and ability to intensify convective currents and thermal mixing [5] [17] [34]-[36]. Multiphysics models that incorporate thermal radiation, entropy generation, and MHD damping illustrate how advanced control parameters can improve heat transfer performance in energy systems [37]-[39]. Meanwhile, parametric studies using response surface methodologies and sensitivity analysis offer quantitative strategies for optimization across varying geometric, fluidic, and magnetic configurations [40]-[42]. Building upon these insights, recent simulations have focused on zigzag wall structures, ferrofluids, and rotating elements to further explore the interplay between geometry, nanofluid properties, and external forces [43] [44]. The numerically investigation of conjugate mixed convection heat transfer in a lid-driven cavity featuring a spinning heat-generating solid cylinder to analyze thermal performance enhance-

ments [45].

In this context, the current study contributes to the literature by numerically investigating MHD-driven conjugate free convection of Cu-$H_2O$ nanofluid within an inclined trapezoidal enclosure featuring a corrugated top wall and internally heat-generating star-shaped copper obstacles. The research aims to uncover how variations in Rayleigh number, Hartmann number, and nanoparticle volume fraction affect flow dynamics and heat transfer, thereby offering design guidelines for efficient thermal management in advanced engineering applications.

## 2. Model Description

The physical model considered in this study consists of a two-dimensional inclined trapezoidal enclosure filled with a Cu–$H_2O$ nanofluid and subjected to free convective heat transfer under the influence of a uniform transverse magnetic field. As shown in Figure 1, the top boundary of the enclosure is sinusoidally corrugated, while the side walls are inclined at a base angle $\gamma$, forming a trapezoidal geometry. Two identical internal star-shaped copper obstacles are embedded symmetrically within the nanofluid domain, each acting as a localized heat source.

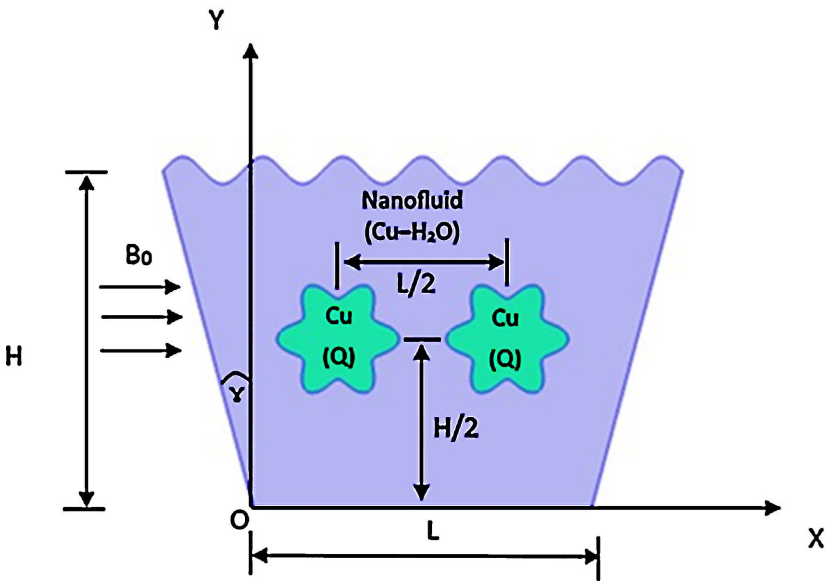


Figure 1. Geometry.

The coupled heat transfer process includes conduction within the solid copper obstacles and convection–conduction within the nanofluid, forming a conjugate heat transfer problem. The nanofluid is assumed to be incompressible and Newtonian, and the flow is driven by buoyancy forces due to internal heating, with the Boussinesq approximation applied to account for density variations.

The governing equations are formulated for mass, momentum, and energy conservation and are solved numerically using the Galerkin finite element method (FEM). The system is subject to the following thermal boundary conditions, summarized in Table 1 and elaborated below:

**Table 1.** Boundary condition.

| Boundary | Condition | Temperature Value |
|---|---|---|
| Top Wavy Wall | Isothermal | $T = T_m$ |
| Bottom Wall | Isothermal | $T = T_m$ |
| Left & Right Walls | Thermal Insulation (Adiabatic) | $n \cdot \nabla T = 0$ |
| Star Obstacles | Internal Heat Source | Volumetric heating $Q$ |

Top Wavy Wall: Maintained at a constant cold temperature $T = T_m$, this boundary facilitates upward thermal diffusion and mimics a cooled surface. Its sinusoidal profile increases surface area, enhancing local heat exchange and promoting complex flow structures such as vortices.

Bottom Wall: Also kept isothermal at the cold reference temperature $T = T_m$, the bottom wall acts as a second cooling surface. The thermal symmetry created by the top and bottom boundaries encourages the rise of heated fluid and the fall of cooled fluid, forming closed-loop natural convection currents.

Left and Right Inclined Walls: These boundaries are thermally insulated, implying zero heat flux across them, mathematically expressed as $n \cdot \nabla T = 0$. This adiabatic condition confines the thermal activity within the interior domain, ensuring that heat transfer is driven purely by internal generation and vertical heat dissipation.

Star-Shaped Obstacles: Each copper obstacle is modeled as an internally heat-generating solid, with uniform volumetric heating characterized by a source term $Q$. These localized heaters represent embedded thermal devices and induce strong buoyancy-driven flows within the surrounding nanofluid, making them critical to the dynamics of the convective patterns observed.

This boundary condition setup ensures a vertically symmetric thermal gradient with dominant internal heating. Combined with the wavy top surface, it produces a highly interactive flow environment ideal for investigating the effect of magnetic field strength, Rayleigh number, and nanoparticle volume fraction on the system's thermal behavior.

## 3. Mathematical Modeling

This study investigates the conjugate magnetohydrodynamic (MHD) free convection within a nanofluid-saturated trapezoidal enclosure containing internal heat-generating star-shaped obstacles. The base fluid is water, while copper (Cu) nanoparticles are dispersed to form the Cu-$H_2O$ nanofluid. The governing physical model incorporates the conservation equations of mass, momentum, and energy under the Boussinesq approximation. The enclosure is subjected to a uniform magnetic field perpendicular to the slanted side, introducing Lorentz force effects on the convective flow.

**Governing Equations:**

Assuming laminar, incompressible, and steady-state flow conditions, the gov-

erning dimensional and non-dimensional equations (1) to (22) are as follows:

$$\frac{\partial u}{\partial x}+\frac{\partial v}{\partial y}=0 \tag{1}$$

$$\rho_{nf}\left(u\frac{\partial u}{\partial x}+v\frac{\partial u}{\partial y}\right)=-\frac{\partial p}{\partial x}+\mu_{nf}\left(\frac{\partial^2 u}{\partial x^2}+\frac{\partial^2 u}{\partial y^2}\right)+\rho_{nf}g\beta_{nf}\left(T-T_c\right)\sin\left(\gamma\right)-\sigma_{nf}\beta_0^2 u \tag{2}$$

$$\rho_{nf}\left(u\frac{\partial v}{\partial x}+v\frac{\partial v}{\partial y}\right)=-\frac{\partial p}{\partial y}+\mu_{nf}\left(\frac{\partial^2 v}{\partial x^2}+\frac{\partial^2 v}{\partial y^2}\right)+\rho_{nf}g\beta_{nf}\left(T-T_c\right)\cos\left(\gamma\right)-\sigma_{nf}\beta_0^2 v \tag{3}$$

$$\rho_{nf}c_{p,nf}\left(u\frac{\partial T}{\partial x}+v\frac{\partial T}{\partial y}\right)=k_{nf}\left(\frac{\partial^2 T}{\partial x^2}+\frac{\partial^2 T}{\partial y^2}\right)+Q \tag{4}$$

Nanofluid Property:

$$\rho_{nf}=\left(1-\phi\right)\rho_f+\phi\rho_s \tag{5}$$

$$\left(\rho c_p\right)_{nf}=\left(1-\phi\right)\left(\rho c_p\right)_f+\phi\left(\rho c_p\right)_s \tag{6}$$

$$\mu_{nf}=\frac{\mu_f}{\left(1-\phi\right)^{2.5}} \tag{7}$$

$$k_{nf}=k_f\left[\frac{k_s+2k_f-2\phi\left(k_f-k_s\right)}{k_s+2k_f+\phi\left(k_f-k_s\right)}\right] \tag{8}$$

$$\beta_{nf}=\frac{\left(1-\phi\right)\rho_f\beta_f+\phi\rho_s\beta_s}{\rho_{nf}} \tag{9}$$

Non-Dimensional Equations:

$$X=\frac{x}{L},Y=\frac{y}{L},U=\frac{uL}{\alpha_f},V=\frac{vL}{\alpha_f},\theta=\frac{T-T_c}{T_h-T_c},P=\frac{pL^2}{\mu_{nf}},\text{Here},\alpha_f=\frac{k_f}{\rho_f c_{p,f}} \tag{10}$$

$$Ra=\frac{g\beta_{nf}\left(T_h-T_c\right)L^3}{\nu_{nf}\alpha_f},Pr=\frac{\nu_f}{\alpha_f},Ha=\beta_0 L\sqrt{\frac{\sigma_{nf}}{\mu_{nf}}},Q^*=\frac{QL^2}{k_{nf}\left(T_h-T_c\right)} \tag{11}$$

$$\frac{\partial U}{\partial X}+\frac{\partial V}{\partial Y}=0 \tag{12}$$

$$U\frac{\partial U}{\partial X}+V\frac{\partial U}{\partial Y}=-\frac{\partial P}{\partial X}+\frac{\mu_{nf}}{\mu_f}\left(\frac{\partial^2 U}{\partial X^2}+\frac{\partial^2 U}{\partial Y^2}\right)+RaPr\frac{\rho_{nf}\beta_{nf}}{\rho_f\beta_f}\theta\sin\left(\gamma\right)-Ha^2U \tag{13}$$

$$U\frac{\partial V}{\partial X}+V\frac{\partial V}{\partial Y}=-\frac{\partial P}{\partial X}+\frac{\mu_{nf}}{\mu_f}\left(\frac{\partial^2 V}{\partial X^2}+\frac{\partial^2 V}{\partial Y^2}\right)+RaPr\frac{\rho_{nf}\beta_{nf}}{\rho_f\beta_f}\theta\cos\left(\gamma\right)-Ha^2U \tag{14}$$

$$U\frac{\partial \theta}{\partial X}+V\frac{\partial \theta}{\partial Y}=\frac{k_{nf}}{k_f}\frac{1}{Pr}\left(\frac{\partial^2 \theta}{\partial X^2}+\frac{\partial^2 \theta}{\partial Y^2}\right)+Q^* \tag{15}$$

Here, $Q^*$ represents the internal heat generation within the star-shaped obstacles

and is scaled using the characteristic temperature difference $\Delta T=T_h-T_c$

Nanofluid Property:

$$\frac{\rho_{nf}}{\rho_f} = (1-\phi) + \phi\frac{\rho_s}{\rho_f} \tag{16}$$

$$\frac{(\rho c_p)_{nf}}{(\rho c_p)_f} = (1-\phi) + \phi\frac{(\rho c_p)_s}{(\rho c_p)_f} \tag{17}$$

$$\frac{\mu_{nf}}{\mu_f} = \frac{1}{(1-\phi)^{2.5}} \tag{18}$$

$$\frac{k_{nf}}{k_f} = \frac{k_s + 2k_f - 2\phi(k_f - k_s)}{k_s + 2k_f + \phi(k_f - k_s)} \tag{19}$$

$$\beta_{nf}\rho_{nf} = (1-\phi)\rho_f\beta_f + \phi\rho_s\beta_s \tag{20}$$

Local Nusselt number ($Nu$) and Average Nusselt number ($Nu_{avg}$) inside the enclosure are assessed and expressed as performance parameters of the current system in the following ways:

$$Nu_{Local} = -\frac{\partial\theta}{\partial n}\bigg|_{\text{Wavy-Wall}} \tag{21}$$

$$\bar{N}u = \frac{1}{L_w}\int_0^{L_w} Nu_{Local}\,\mathrm{d}X = -\frac{1}{L_w}\int_0^{L_w}\frac{\partial\theta}{\partial n}\mathrm{d}X \tag{22}$$

Here, $L_w$ is the arc length of the top wavy wall.

**Thermophysical Parameters**

The thermophysical properties of copper nanoparticles and pure water are summarized in Table 2, while the nanofluid properties for varying volume fractions are detailed in Table 3.

Table 2. Thermophysical properties of pure water and copper nanoparticles.

| Thermophysical Properties | Copper Nanoparticles | Pure Water |
|---|---|---|
| $\rho$ (kg/m$^3$) | 8933 | 996.60 |
| $C_p$ (J/kg·K) | 385 | 4179.20 |
| $k$ (W/m·K) | 401 | 0.6102 |
| $\beta$ (1/K) | $4.99 \times 10^{-5}$ | $2.66 \times 10^{-4}$ |
| $\sigma$ (1/Ω·m) | $5.96 \times 10^{-7}$ | $5.50 \times 10^{-6}$ |

Table 2 shows the thermophysical properties of copper nanoparticles and pure water. Copper has high density, thermal, and electrical conductivity, making it ideal for enhancing heat transfer. In contrast, water has a much higher specific heat and expansion coefficient, supporting strong buoyancy effects.

Table 3 presents nanofluid properties at different nanoparticle volume fractions. As copper content increases, thermal conductivity, viscosity, and density rise, while specific heat and thermal expansion decrease. This highlights the trade-off between improved heat transfer and fluid resistance.

Table 3. Properties of nanofluid.

| Property | Unit | Volume Fraction of Nanoparticles | | |
|---|---|---|---|---|
| | | 0.01 | 0.02 | 0.03 |
| Density ($\rho$) | kg/m$^3$ | 1076.00 | 1155.30 | 1234.70 |
| Specific heat ($C_p$) | J/kg·K | 3864.20 | 3592.50 | 3355.70 |
| Thermal conductivity ($k$) | W/m·K | 0.62861 | 0.64739 | 0.66655 |
| Dynamic viscosity ($\mu$) | kg/m·s | $8.7552 \times 10^{-4}$ | $8.9803 \times 10^{-4}$ | $9.2135 \times 10^{-4}$ |
| Electric conductivity ($\sigma$) | $\Omega^{-1}\cdot m^{-1}$ | $5.6667 \times 10^{-6}$ | $5.8367 \times 10^{-6}$ | $6.0103 \times 10^{-6}$ |
| Thermal diffusivity ($\alpha$) | m$^2$/s | $1.4651 \times 10^{-7}$ | $1.4651 \times 10^{-7}$ | $1.465 \times 10^{-7}$ |
| Volumetric expansion ($\beta$) | K$^{-1}$ | $2.4806 \times 10^{-4}$ | $2.3258 \times 10^{-4}$ | $2.191 \times 10^{-4}$ |

## 4. Results and Discussion

### 4.1. Verification

The streamline comparison in Figure 2 demonstrates strong agreement between the present numerical study and the results from Ref. [45].

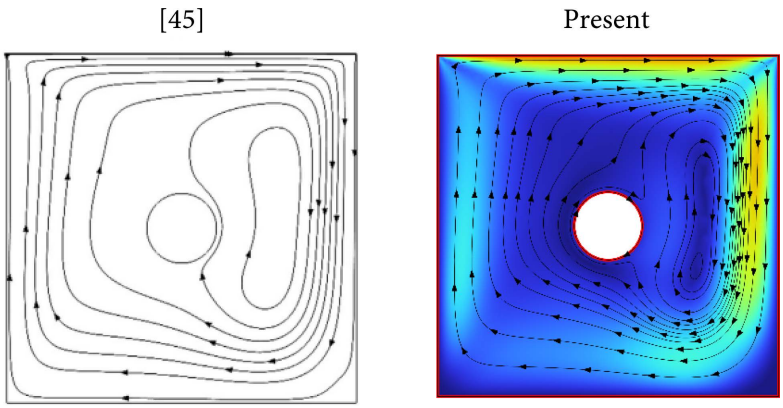


Figure 2. Comparison of the Streamline in the present study and the Ref. [45].

Both streamlines illustrate a primary circulation cell formed due to the lid-driven motion and the influence of the central rotating heat-generating cylinder. In Ref. [45], the streamlines show symmetrical vortex structures and steady flow separation zones near the cylinder, while the present study captures similar flow features with enhanced clarity and color-coded velocity magnitudes, validating the computational model. This visual correlation supports the reliability and accuracy of the present simulation in capturing conjugate mixed convection dynamics.

### 4.2. Discussion

To visualize the effects of nanoparticle volume fraction, magnetic field strength, and thermal buoyancy on convective flow and heat transfer behavior, Figure 3-8 present detailed contour plots of velocity and temperature distributions. These figures capture the flow dynamics and thermal gradients within the nanofluid-

filled trapezoidal enclosure for three nanoparticle volume fractions ($\phi = 0.01$, 0.02, and 0.03), under varying Rayleigh numbers ($Ra = 10^3$ to $10^6$) and Hartmann numbers ($Ha$ = 15 and 50). The contours highlight how thermal and hydrodynamic fields evolve due to internal heat generation from star-shaped obstacles, and they illustrate the interplay between magnetic damping, nanoparticle-enhanced thermal conductivity, and buoyancy-driven convection.

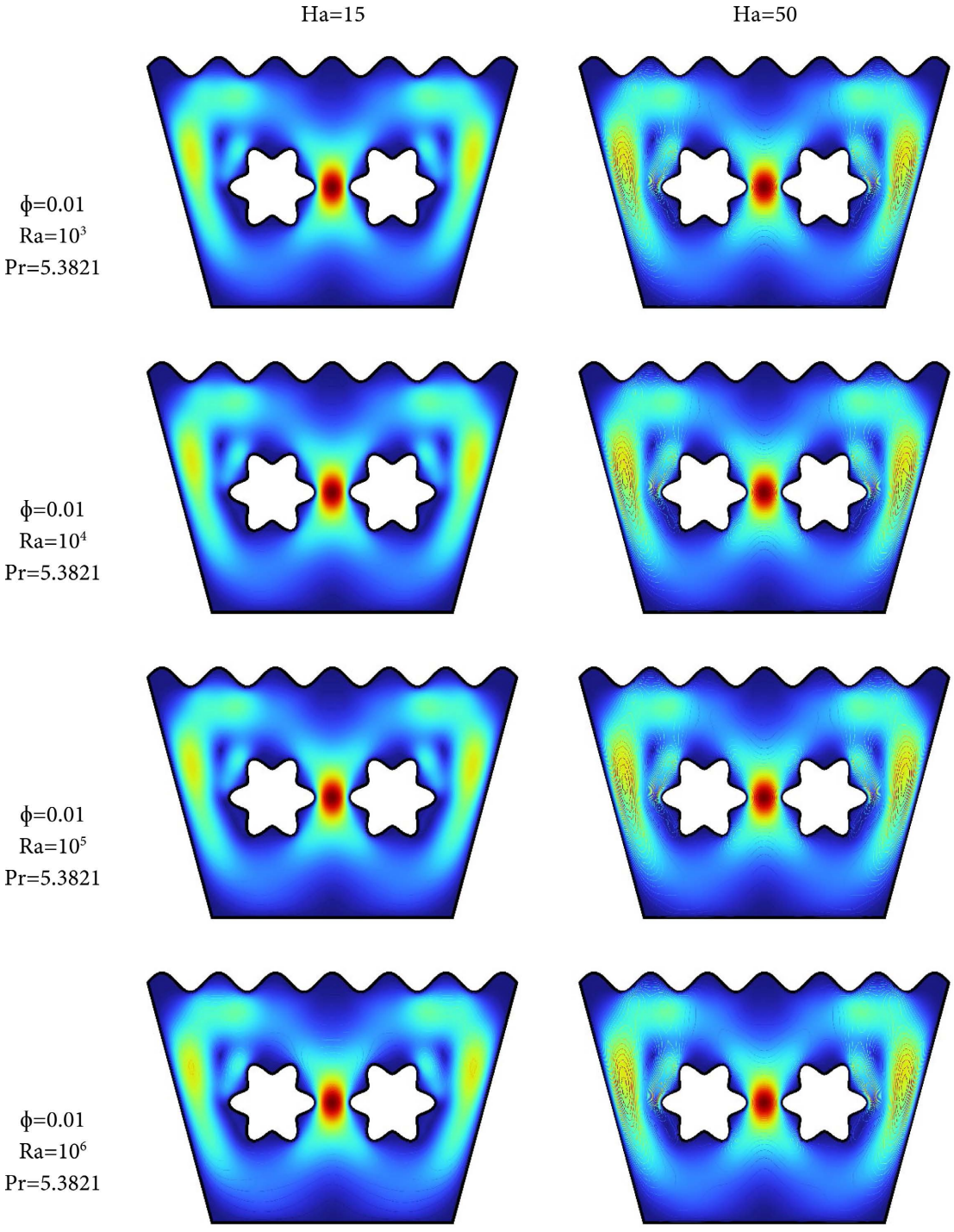


**Figure 3.** Velocity contour for nanoparticle volume fraction $\phi = 0.01$.

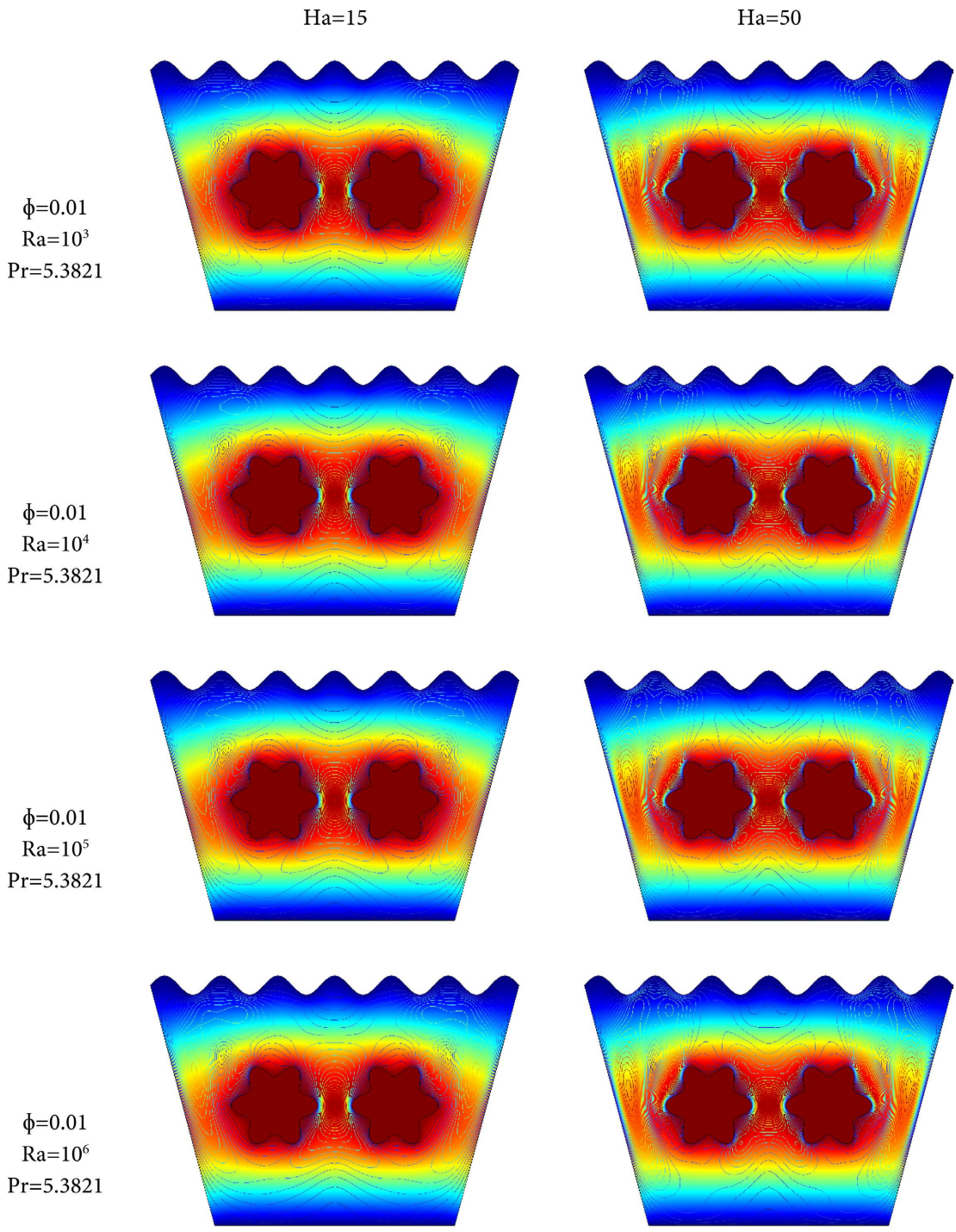


**Figure 4.** Temperature contour for nanoparticle volume fraction $\phi = 0.01$.

**Figure 3** and **Figure 4** display the velocity and temperature contours for $\phi = 0.01$, at four Rayleigh numbers ($10^3$ to $10^6$) and two Hartmann numbers ($Ha = 15$ and 50). At low $Ra$ ($10^3$), the flow is weak and mostly conduction-dominated, with nearly parallel isotherms and minimal vortex formation. As $Ra$ increases, buoyancy becomes more significant, leading to stronger circulation and distorted temperature lines. At $Ha = 15$, velocity fields show more developed vortices compared

to *Ha* = 50, where the magnetic field dampens flow intensity. The temperature fields also become more stratified at high *Ra*, with thinner boundary layers near the heated obstacles.

Figure 5 and Figure 6 correspond to $\phi$ = 0.02. An increase in nanoparticle concentration leads to enhanced thermal conductivity, slightly strengthening the thermal gradients and flow strength at comparable *Ra* and *Ha* values. Compared

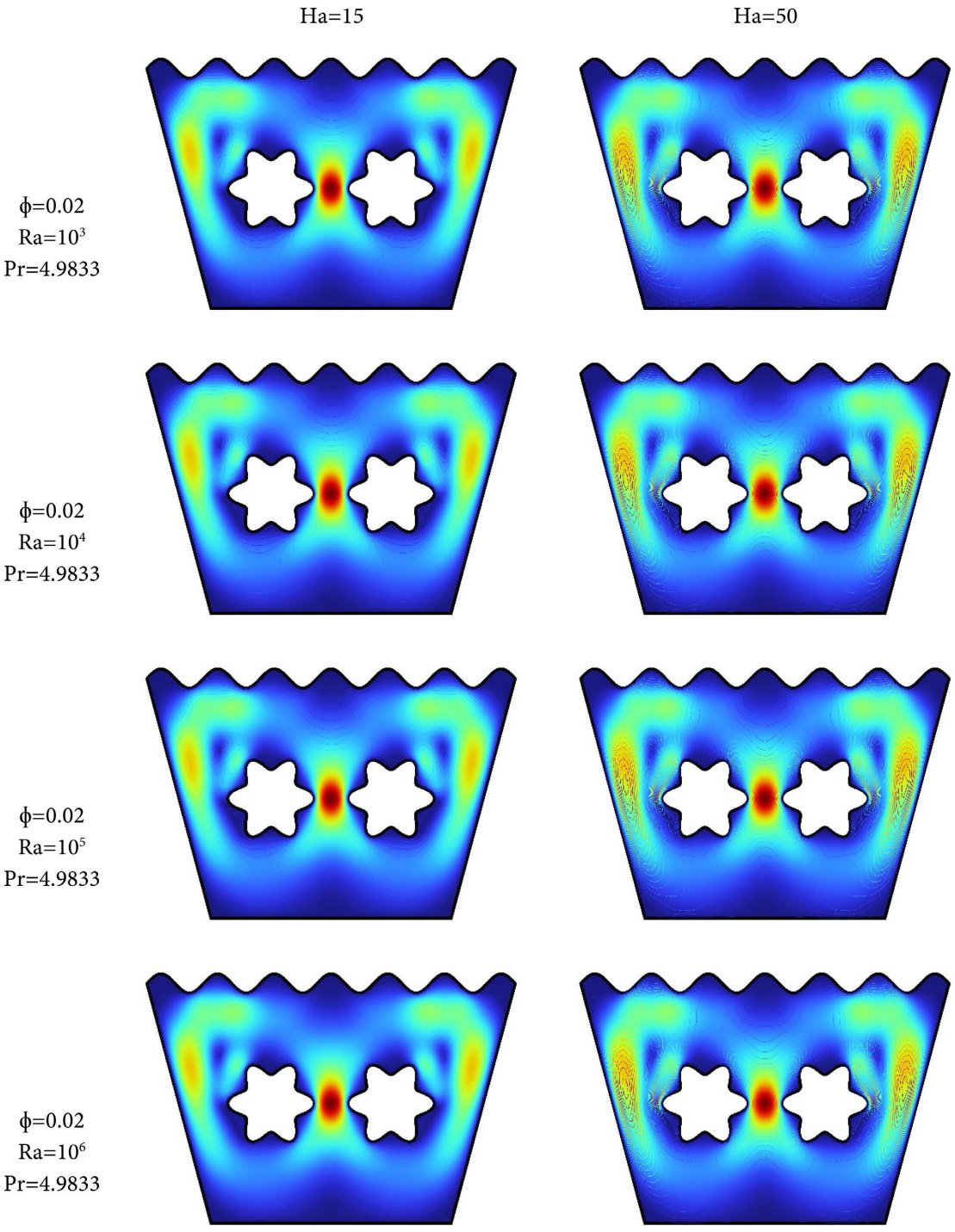


**Figure 5.** Velocity contour for nanoparticle volume fraction $\phi$ = 0.02.

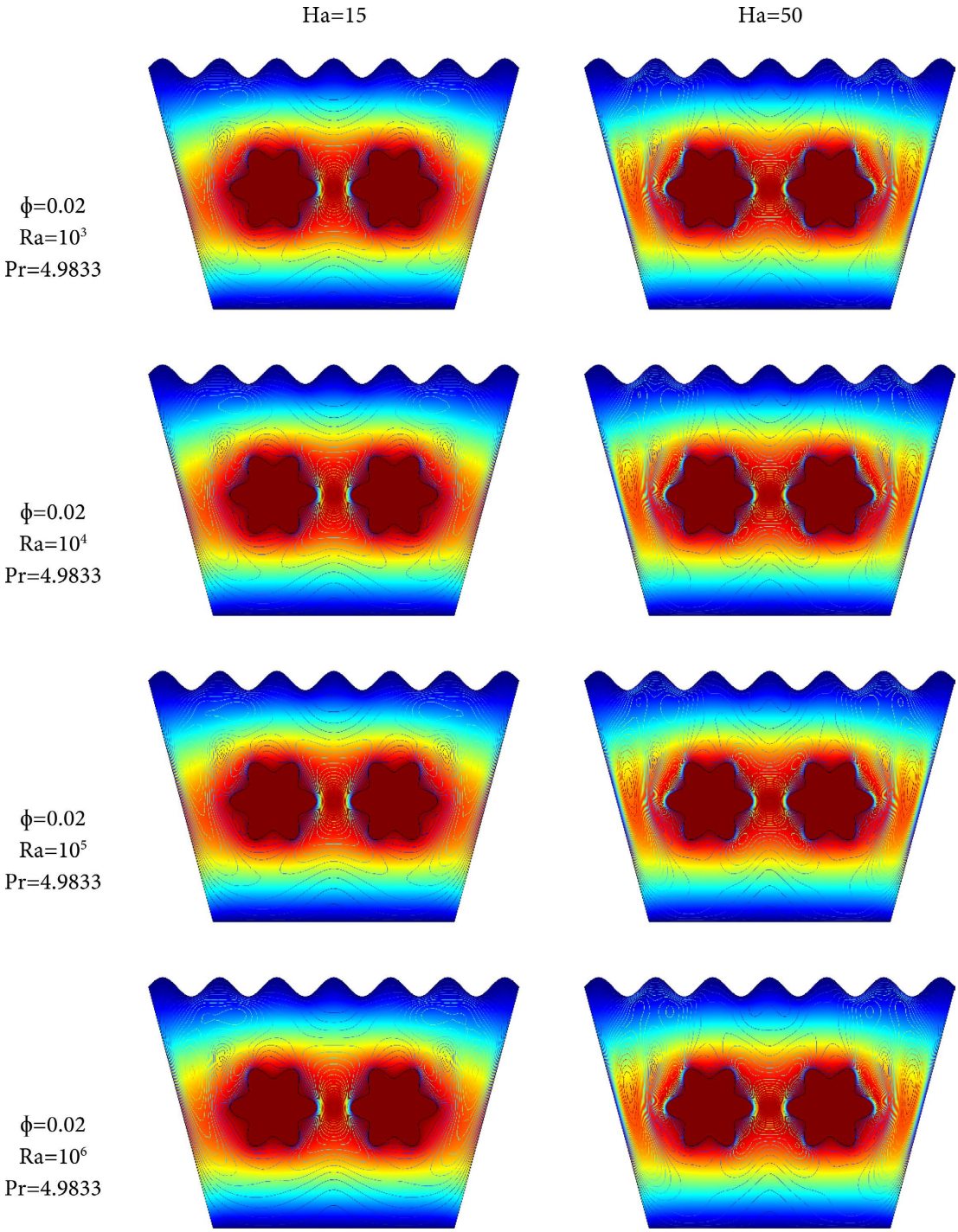


**Figure 6.** Temperature contour for nanoparticle volume fraction $\phi = 0.02$.

to $\phi = 0.01$, vortex structures become more intense at $Ra = 10^5$ and $10^6$, and isotherms near the heated star-shaped obstacles become steeper, indicating better heat dissipation. Again, higher Hartmann number ($Ha = 50$) suppresses flow circulation due to increased Lorentz force, especially at low $Ra$.

Figure 7 and Figure 8 represent the highest nanoparticle volume fraction $\phi = 0.03$. The velocity contours reveal further strengthening of vortices and larger

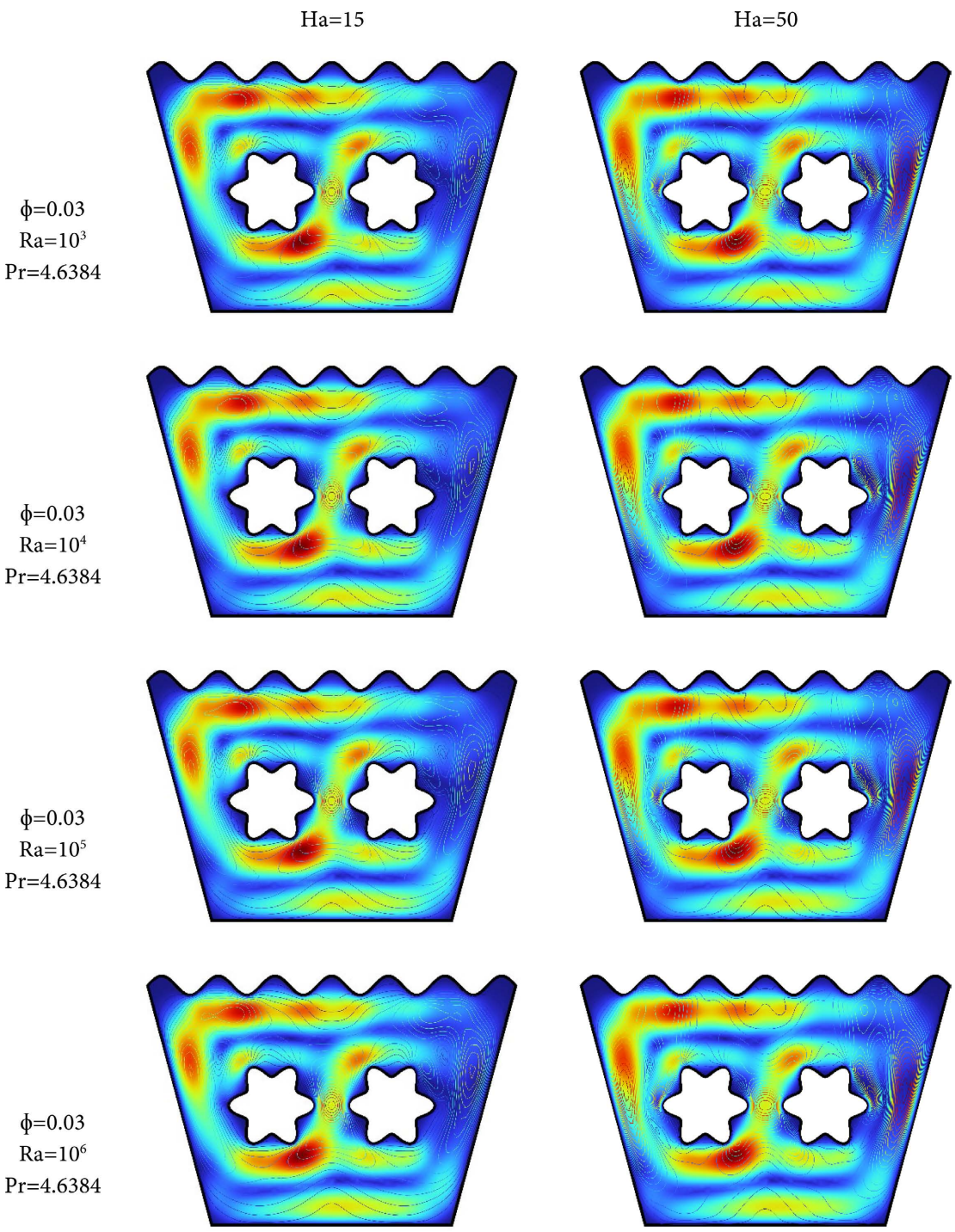


**Figure 7.** Velocity contour for nanoparticle volume fraction $\phi = 0.03$.

recirculation zones at high Ra, particularly for $Ha = 15$. The increased thermal conductivity of the nanofluid at this concentration promotes stronger convection. However, the $Ha = 50$ cases consistently show reduced flow activity, confirming that the magnetic field hinders buoyancy-driven motion. The temperature contours illustrate sharper thermal gradients near the star-shaped heat sources and thinner thermal boundary layers as *Ra* increases.

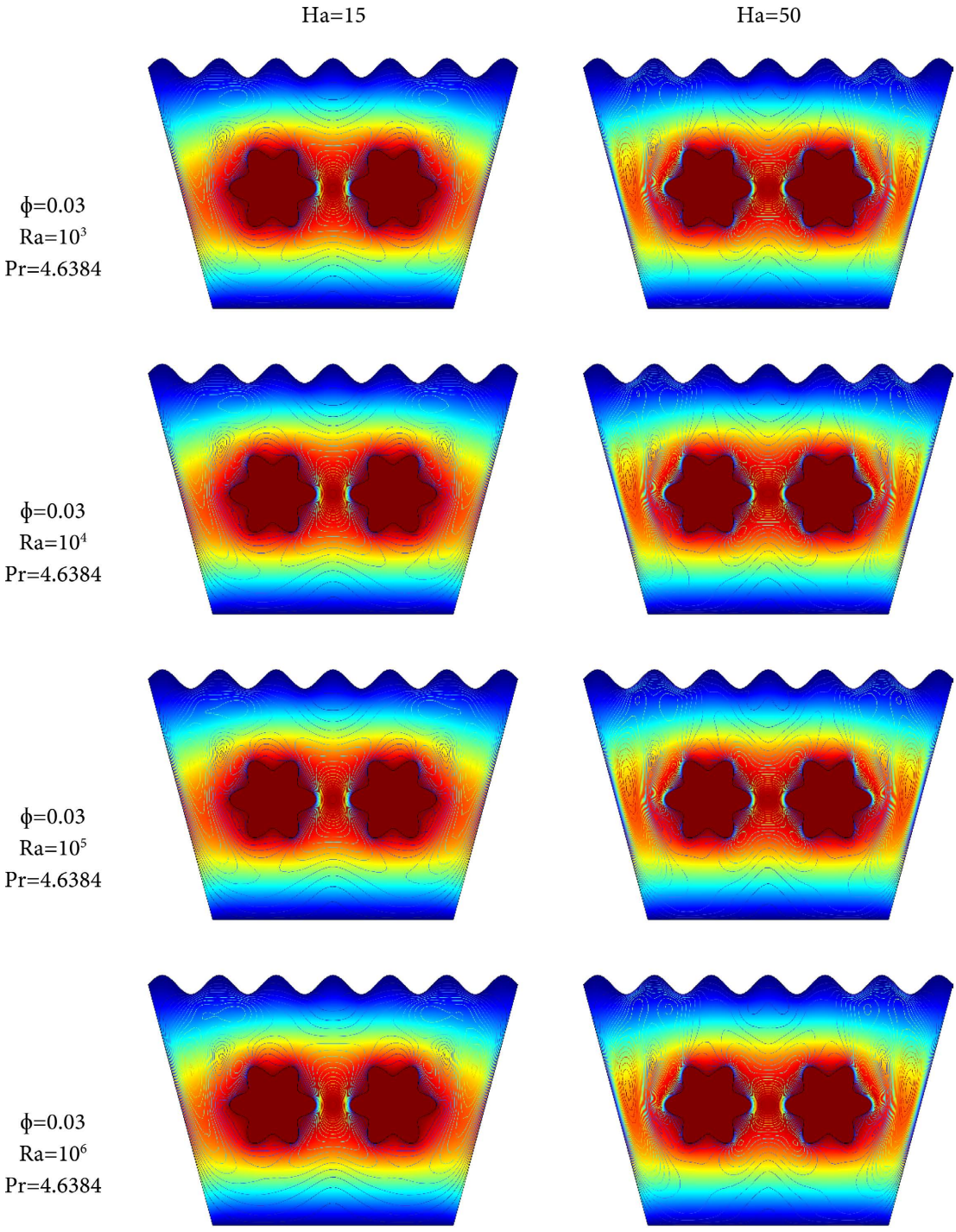


**Figure 8.** Temperature contour for nanoparticle volume fraction $\phi = 0.03$.

**Figures 3-8** observations are:

1) Increasing *Ra* enhances natural convection, visible through intensified vortex size and sharper isotherms.

2) Higher nanoparticle volume fractions ($\phi$) improve heat transfer by increasing thermal conductivity and modifying flow structure.

3) Stronger magnetic fields (higher *Ha*) consistently suppress fluid motion, re-

ducing convective heat transfer and enhancing conduction dominance.

4) The interaction between nanoparticle loading and magnetic damping is critical in optimizing heat transfer in MHD nanofluid systems.

To comprehensively understand the thermofluid behavior inside the trapezoidal nanofluid-filled enclosure under magnetic field influence, a parametric study was conducted by varying the Rayleigh number ($Ra$), Hartmann number ($Ha$), and nanoparticle volume fraction ($\phi$). The results, summarized in Tables 4-9, present the corresponding variations in Nusselt number ($Nu$) and the average nanofluid temperature ($T_{avf}$). These tables provide critical insights into how buoyancy-driven convection, magnetic damping, and enhanced thermal conductivity due to nanoparticles interact to influence heat transfer performance and thermal stability of the system.

Tables 4-9 collectively illustrate the influence of Rayleigh number ($Ra$), Hartmann number ($Ha$), and nanoparticle volume fraction ($\phi$) on the convective heat transfer rate (Nusselt number, $Nu$) and the average nanofluid temperature ($T_{avf}$).

Table 4. $Nu$ and $T_{avf}$ When $\phi = 0.01$, $Pr = 5.3821$ and $Ha = 15$.

| $Ra$ (Rayleigh Number) | $Nu$ (Nusselt Number) | $T_{avf}$ (Average Temperature of Nano Fluid) |
|---|---|---|
| $10^3$ | 0.86665 | 0.0094650 |
| $10^4$ | 2.51720 | 0.0094640 |
| $10^5$ | 3.10980 | 0.0094518 |
| $10^6$ | 3.26330 | 0.0090756 |

Table 5. $Nu$ and $T_{avf}$ When $\phi = 0.01$, $Pr = 5.3821$ and $Ha = 50$.

| $Ra$ (Rayleigh Number) | $Nu$ (Nusselt Number) | $T_{avf}$ (Average Temperature of Nano Fluid) |
|---|---|---|
| $10^3$ | 0.86665 | 0.0094651 |
| $10^4$ | 2.51720 | 0.0094648 |
| $10^5$ | 3.10950 | 0.0094612 |
| $10^6$ | 3.18960 | 0.0094055 |

Table 6. $Nu$ and $T_{avf}$ When $\phi = 0.02$, $Pr = 4.9833$ and $Ha = 15$.

| $Ra$ (Rayleigh Number) | $Nu$ (Nusselt Number) | $T_{avf}$ (Average Temperature of Nano Fluid) |
|---|---|---|
| $10^3$ | 0.87357 | 0.0091905 |
| $10^4$ | 2.5762 | 0.0091896 |
| $10^5$ | 3.2003 | 0.0091788 |
| $10^6$ | 3.3454 | 0.0088667 |

Table 7. $Nu$ and $T_{avf}$ When $\phi = 0.02$, $Pr = 4.9833$ and $Ha = 50$.

| $Ra$ (Rayleigh Number) | $Nu$ (Nusselt Number) | $T_{avf}$ (Average Temperature of Nano Fluid) |
|---|---|---|
| $10^3$ | 0.87357 | 0.0091906 |
| $10^4$ | 2.57620 | 0.0091903 |
| $10^5$ | 3.20000 | 0.0091871 |
| $10^6$ | 3.28380 | 0.0091390 |

Table 8. $Nu$ and $T_{avf}$ When $\phi = 0.03$, $Pr = 4.6384$ and $Ha = 15$.

| $Ra$ (Rayleigh Number) | $Nu$ (Nusselt Number) | $T_{avf}$ (Average Temperature of Nano Fluid) |
|---|---|---|
| $10^3$ | 0.88034 | 0.0089263 |
| $10^4$ | 2.63570 | 0.0089254 |
| $10^5$ | 3.29250 | 0.0089159 |
| $10^6$ | 3.43160 | 0.0086564 |

Table 9. $Nu$ and $T_{avf}$ When $\phi = 0.03$, $Pr = 4.6384$ and $Ha = 50$.

| $Ra$ (Rayleigh Number) | $Nu$ (Nusselt Number) | $T_{avf}$ (Average Temperature of Nano Fluid) |
|---|---|---|
| $10^3$ | 0.88034 | 0.0089263 |
| $10^4$ | 2.63570 | 0.0089261 |
| $10^5$ | 3.29220 | 0.0089232 |
| $10^6$ | 3.38020 | 0.0088816 |

Across all cases, increasing the Rayleigh number ($Ra$) enhances the Nusselt number ($Nu$), indicating stronger convection. When the Hartmann number ($Ha$) is low (15), $Nu$ is consistently higher and the average nanofluid temperature ($T_{avf}$) lower, compared to high $Ha$ (50), due to reduced magnetic damping. Increasing nanoparticle volume fraction ($\phi$) from 0.01 to 0.03 improves heat transfer, as reflected by rising $Nu$ and falling $T_{avf}$. However, this improvement is more effective at low $Ha$, where buoyancy-driven flows are less restricted. Overall, optimal thermal performance is achieved with high $\phi$ and low $Ha$.

**Overall Observations:**

1) $Nu$ increases with higher $Ra$ and $\phi$, and decreases with higher $Ha$.

2) $T_{avf}$ decreases with increasing $Ra$ and $\phi$, and increases with stronger $Ha$.

3) The optimal thermal performance is achieved at high $Ra$ and high $\phi$ with moderate $Ha$.

Figures 9-11 present a comparative analysis of the Nusselt number ($Nu$) as a function of Rayleigh number ($Ra$) for different Hartmann numbers ($Ha = 15$ and $Ha = 50$) under varying nanoparticle volume fractions ($\phi = 0.01$, 0.02, and 0.03). These figures aim to assess the influence of magnetic field strength and nanopar-

ticle loading on the convective heat transfer performance of a nanofluid-filled trapezoidal cavity containing internal heat sources. The Nusselt number is a key indicator of convective heat transfer, and its variation with *Ra*, *Ha*, and $\phi$ provides insights into optimizing thermal performance in magnetohydrodynamic (MHD) systems.

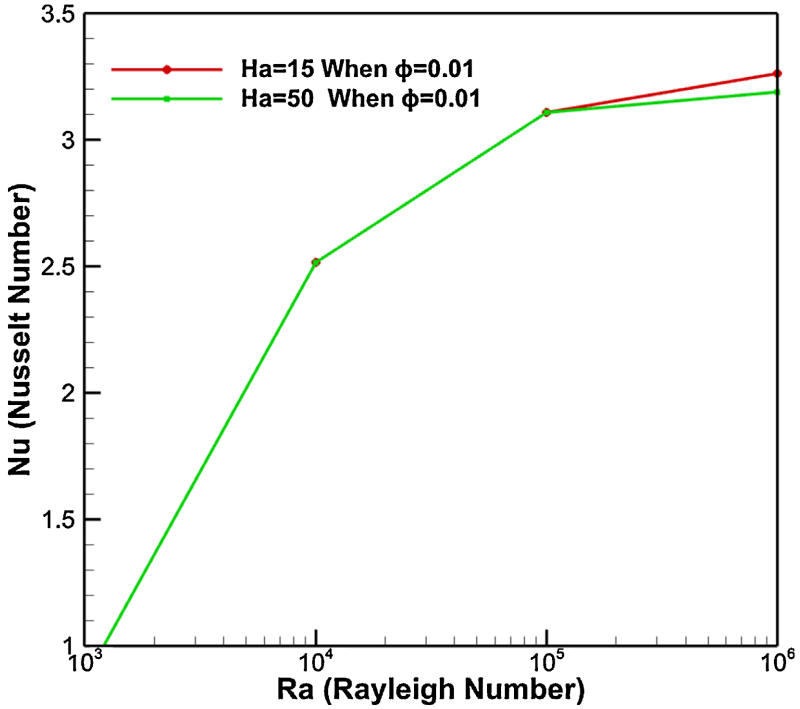


Figure 9. *Nu* vs *Ra* When $\phi = 0.01$, $Pr = 5.3821$, $Ha = 15$ and $Ha = 50$.

**Figure 9:** The Nusselt number increases with *Ra*, confirming enhanced heat transfer due to stronger buoyancy-driven convection. For both $Ha = 15$ and $Ha = 50$, the increase in *Nu* is nonlinear, with more significant gains at higher *Ra*. $Ha = 15$ consistently yields higher *Nu* values than $Ha = 50$, indicating that a weaker magnetic field imposes less damping on flow motion, thus allowing better convective transport.

**Figure 10:** A similar trend is observed where *Nu* rises with *Ra*, and $Ha = 15$ outperforms $Ha = 50$. The inclusion of more nanoparticles slightly raises the *Nu* across the *Ra* range compared to $\phi = 0.01$, showcasing the beneficial effect of enhanced thermal conductivity. However, magnetic suppression becomes more noticeable as $\phi$ increases, emphasizing the trade-off between magnetic damping and nanoparticle-induced enhancement.

**Figure 11:** This case shows the highest *Nu* values overall, confirming that greater nanoparticle concentration substantially improves heat transfer. Yet, the gap between $Ha = 15$ and $Ha = 50$ is still evident, reaffirming the inhibitory influence of stronger magnetic fields on convection. This figure highlights that while nanoparticle addition enhances *Nu*, optimizing *Ha* is crucial to maximizing thermal efficiency.

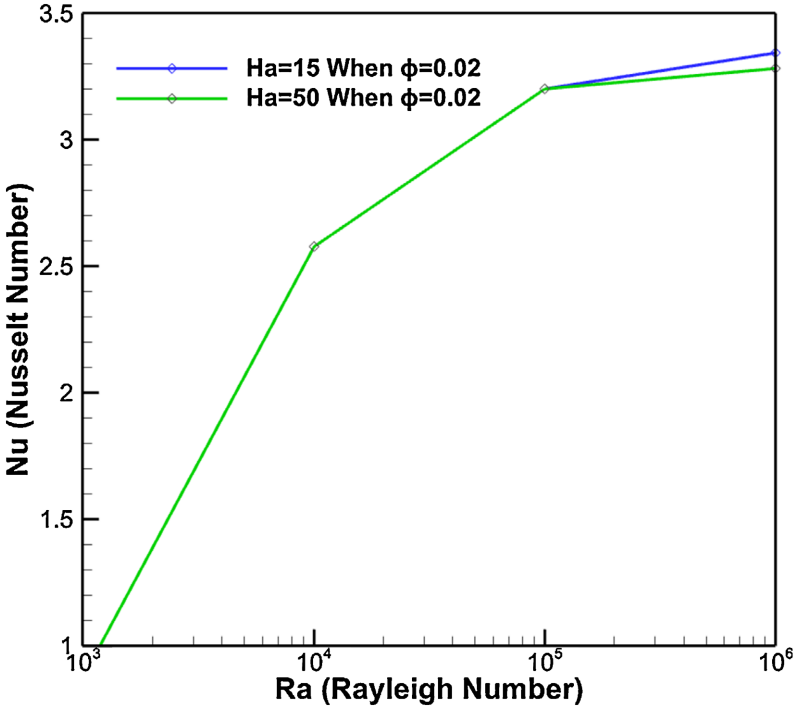


Figure 10. *Nu* vs *Ra* When $\phi = 0.02$, $Pr = 4.9833$, $Ha = 15$ and $Ha = 50$.

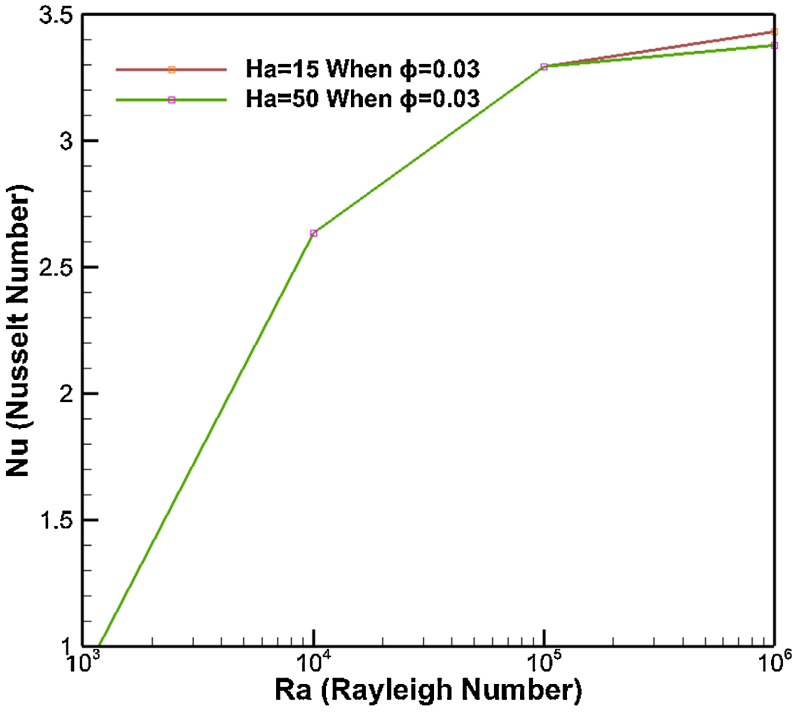


Figure 11. *Nu* vs *Ra* When $\phi = 0.03$, $Pr = 4.6384$, $Ha = 15$ and $Ha = 50$.

Together, these figures underscore that increasing *Ra* and $\phi$ boosts heat transfer, while higher *Ha* values tend to suppress it. Therefore, a balanced design considering both nanoparticle loading and magnetic field strength is essential for optimal MHD thermal system performance.

## 5. Conclusions

This study systematically analyzed the convective heat transfer behavior of Cu-water nanofluid in an inclined trapezoidal enclosure featuring a wavy top wall and internally placed star-shaped heat sources under the influence of a magnetic field. Through parametric variation of Rayleigh numbers ($10^3$ - $10^6$), Hartmann numbers (15, 50), and nanoparticle volume fractions (0.01 - 0.03), and employing the finite element method, the investigation highlighted how geometric complexity and magnetic control collectively influence thermal transport and fluid flow characteristics.

**Key Findings:**

1) Rayleigh number enhancement consistently increased the Nusselt number and promoted stronger convective currents across all nanoparticle concentrations and magnetic field strengths.

2) Higher nanoparticle volume fractions improved the thermal conductivity of the fluid and elevated convective heat transfer, with $\phi = 0.03$ yielding the highest performance.

3) Magnetic field application ($Ha$) suppressed convection due to Lorentz force damping, resulting in reduced Nusselt numbers, especially at higher $Ha = 50$ compared to $Ha = 15$.

4) Velocity and temperature contours revealed that higher $Ra$ and lower $Ha$ produce more vigorous circulation and better thermal mixing, while increasing $\phi$ reduced the average fluid temperature due to enhanced thermal transport.

5) A maximum enhancement of heat transfer was observed at $Ra = 10^6$, $\phi = 0.03$, and $Ha = 15$, demonstrating the synergistic effect of thermal conductivity and buoyancy dominance under weaker magnetic damping.

**Future Work:**

To extend the current research, the following directions are suggested:

1) Investigate the transient behavior of nanofluid convection in time-dependent heating applications.

2) Incorporate non-Newtonian nanofluids and hybrid nanoparticles to assess advanced thermal performance.

3) Evaluate the effects of variable wall temperature, different obstacle shapes, or moving heat sources for more complex real-world modeling.

4) Explore machine learning-based surrogate models to predict optimal configurations with reduced computational cost.

5) Consider the impact of three-dimensional geometries and inclination angles to improve generalization for practical designs.

The findings demonstrate that integrating Cu-water nanofluids with star-shaped internal heaters in a wavy top trapezoidal cavity under magnetic influence provides a highly effective approach for thermal enhancement. By fine-tuning key parameters Rayleigh number, nanoparticle volume fraction, and Hartmann number, the system achieves improved convective mixing and enhanced heat transfer while maintaining controlled flow behavior. The complex geometry amplifies

thermal performance through increased surface area and strategic flow disruption. This makes it particularly well-suited for applications like data center cooling and compact heat exchangers, where managing localized heat buildup is essential for maintaining reliability and operational efficiency.

## Acknowledgements

We sincerely thank the Department of Mathematics, DUET, Gazipur, for their continuous support, guidance, and facilities throughout this research work.

## Conflicts of Interest

The authors declare no conflicts of interest regarding the publication of this paper.

## References

[1] Nadeem, S., Arif, M., Ullah, I. and Alzabut, J. (2025) MHD Natural Convection of Nanofluid Flow Using a Corrugated Permeable Medium within Corrugated Circular Cavity. *Journal of Thermal Analysis and Calorimetry*, **150**, 5697-5724. https://doi.org/10.1007/s10973-025-14032-y

[2] Hameed, R.H., Hussein, R.A., Al-Salami, Q.H., Alomari, M.A., Hassan, A.M., Alyousuf, F.Q.A., *et al.* (2025) Free Convection Investigation for a Casson-Based Cu-$H_2O$ Nanofluid in Semi Parabolic Enclosure with Corrugated Cylinder. *Heliyon*, **11**, e40960. https://doi.org/10.1016/j.heliyon.2024.e40960

[3] Mahmuda, S. and Ali, M.M. (2025) MHD Free Convection Flow of Nanofluids Inside a Flush Mounted Heated Square Cavity Containing a Heat Conducting Triangular Cylinder. *International Journal of Applied and Computational Mathematics*, **11**, Article No. 34. https://doi.org/10.1007/s40819-025-01839-4

[4] Habiba, U., Hudha, M.N., Neogi, B., Islam, S. and Rahman, M.M. (2025) Numerical Exploration on N-Decane Nanofluid Based MHD Mixed Convection in a Lid Driven Cavity: Impact of Magnetic Field and Thermal Radiation. *International Journal of Thermofluids*, **27**, Article 101209. https://doi.org/10.1016/j.ijft.2025.101209

[5] Ziaur, R.M., Azad, A.K. and Rahman, M.M. (2024) Sensitivity Study on Convective Heat Transfer in a Driven Cavity with Star-Shaped Obstacle and Hybrid Nanofluid Using Response Surface Methodology. *Heliyon*, **10**, e37440. https://doi.org/10.1016/j.heliyon.2024.e37440

[6] Qasem, N.A.A., Abderrahmane, A., Khetib, Y., Rawa, M., Abdulkadhim, A., Eldin, S.M., *et al.* (2023) Mixed Convection within Trapezoidal-Wavy Enclosure Filled with Nano-Encapsulated Phase Change Material: Effect of Magnetohydrodynamics and Wall Waviness. *Case Studies in Thermal Engineering*, **42**, Article 102726. https://doi.org/10.1016/j.csite.2023.102726

[7] Alipour, N., Jafari, B. and Hosseinzadeh, K. (2023) Optimization of Wavy Trapezoidal Porous Cavity Containing Mixture Hybrid Nanofluid (Water/Ethylene Glycol Go-$Al_2O_3$) by Response Surface Method. *Scientific Reports*, **13**, Article No. 1635. https://doi.org/10.1038/s41598-023-28916-2

[8] Maneengam, A., Bouzennada, T., Abderrahmane, A., Ghachem, K., Kolsi, L., Younis, O., *et al.* (2022) Numerical Study of 3D MHD Mixed Convection and Entropy Generation in Trapezoidal Porous Enclosure Filled with a Hybrid Nanofluid: Effect of Zigzag Wall and Spinning Inner Cylinder. *Nanomaterials*, **12**, Article 1974. https://doi.org/10.3390/nano12121974

[9] Hirpho, M. (2021) Mixed Convection of Casson Fluid in a Differentially Heated Bottom Wavy Wall. *Heliyon*, **7**, e07361. https://doi.org/10.1016/j.heliyon.2021.e07361

[10] Ahmad, H., Mahmood, R., Hafeez, M.B., Hussain Majeed, A., Askar, S. and Shahzad, H. (2022) Thermal Visualization of Ostwald-De Waele Liquid in Wavy Trapezoidal Cavity: Effect of Undulation and Amplitude. *Case Studies in Thermal Engineering*, **29**, Article 101698. https://doi.org/10.1016/j.csite.2021.101698

[11] Olayemi, O.A., Isiaka, M., Al-Farhany, K., Alomari, M.A., Ismael, M.A. and Oyedepo, S.O. (2022) Numerical Analysis of Natural Convection in a Concentric Trapezoidal Enclosure Filled with a Porous Medium. *International Journal of Engineering Research in Africa*, **61**, 129-150. https://doi.org/10.4028/p-jza9vq

[12] Uddin, M.J. and Rasel, S.K. (2019) Numerical Analysis of Natural Convective Heat Transport of Copper Oxide-Water Nanofluid Flow Inside a Quadrilateral Vessel. *Heliyon*, **5**, e01757. https://doi.org/10.1016/j.heliyon.2019.e01757

[13] Sompong, P. and Witayangkurn, S. (2013) Natural Convection in a Trapezoidal Enclosure with Wavy Top Surface. *Journal of Applied Mathematics*, **2013**, Article ID: 840632. https://doi.org/10.1155/2013/840632

[14] Mondal, P. and Mahapatra, T.R. (2020) Minimization of Entropy Generation Due to MHD Double Diffusive Mixed Convection in a Lid Driven Trapezoidal Cavity with Various Aspect Ratios. *Nonlinear Analysis: Modelling and Control*, **25**, 545-563. https://doi.org/10.15388/namc.2020.25.16774

[15] Hossain, M.S., Alim, M.A. and Andallah, L.S. (2020) Finite Element Analysis of Magnetohydrodynamic Mixed Convection in a Lid-Driven Trapezoidal Enclosure Having Heated Triangular Block. *American Journal of Computational Mathematics*, **10**, 441-459. https://doi.org/10.4236/ajcm.2020.103025

[16] Abderrahmane, A., Younis, O., Al-Khaleel, M., Laidoudi, H., Akkurt, N., Guedri, K., *et al.* (2022) 2D MHD Mixed Convection in a Zigzag Trapezoidal Thermal Energy Storage System Using NEPCM. *Nanomaterials*, **12**, Article 3270. https://doi.org/10.3390/nano12193270

[17] Bilal, S., Shah, I.A., Ghachem, K., Aydi, A. and Kolsi, L. (2023) Heat Transfer Enhancement of MHD Natural Convection in a Star-Shaped Enclosure, Using Heated Baffle and MWCNT-Water Nanofluid. *Mathematics*, **11**, Article 1849. https://doi.org/10.3390/math11081849

[18] Ibrahim, W. and Hirpho, M. (2021) Finite Element Analysis of Mixed Convection Flow in a Trapezoidal Cavity with Non-Uniform Temperature. *Heliyon*, **7**, e05933. https://doi.org/10.1016/j.heliyon.2021.e05933

[19] Suresh Reddy, E. and Panda, S. (2022) Heat Transfer of *MHD* Natural Convection Casson Nanofluid Flows in a Wavy Trapezoidal Enclosure. *The European Physical Journal Special Topics*, **231**, 2733-2747. https://doi.org/10.1140/epjs/s11734-022-00609-3

[20] Hirpho, M. and Ibrahim, W. (2022) Mixed Convection Heat Transfer of a Hybrid Nanofluid in a Trapezoidal Prism with an Adiabatic Circular Cylinder. *Mathematical Problems in Engineering*, **2022**, Article ID: 8170224. https://doi.org/10.1155/2022/8170224

[21] Hussein, A.K., Hamzah, H.K., Ali, F.H. and Kolsi, L. (2020) Mixed Convection in a Trapezoidal Enclosure Filled with Two Layers of Nanofluid and Porous Media with a Rotating Circular Cylinder and a Sinusoidal Bottom Wall. *Journal of Thermal Analysis and Calorimetry*, **141**, 2061-2079. https://doi.org/10.1007/s10973-019-08963-6

[22] Selimefendigil, F. (2018) Natural Convection in a Trapezoidal Cavity with an Inner Conductive Object of Different Shapes and Filled with Nanofluids of Different Na-

noparticle Shapes. *Iranian Journal of Science and Technology, Transactions of Mechanical Engineering*, **42**, 169-184. https://doi.org/10.1007/s40997-017-0083-3

[23] Mahmood, R., Khan, Y., Rahman, N., Majeed, A.H., Alameer, A. and Faraz, N. (2022) Numerical Computations of Entropy Generation and MHD Ferrofluid Filled in a Closed Wavy Configuration: Finite Element Based Study. *Frontiers in Physics*, **10**, Article 916394. https://doi.org/10.3389/fphy.2022.916394

[24] Job, V.M., Gunakala, S.R. and Chamkha, A.J. (2022) Numerical Investigation of Unsteady MHD Mixed Convective Flow of Hybrid Nanofluid in a Corrugated Trapezoidal Cavity with Internal Rotating Heat-Generating Solid Cylinder. *The European Physical Journal Special Topics*, **231**, 2661-2668. https://doi.org/10.1140/epjs/s11734-022-00604-8

[25] Alshuraiaan, B. and Pop, I. (2021) Numerical Simulation of Mixed Convection in a Lid-Driven Trapezoidal Cavity with Flexible Bottom Wall and Filled with a Hybrid Nanofluid. *The European Physical Journal Plus*, **136**, Article No. 580. https://doi.org/10.1140/epjp/s13360-021-01349-4

[26] Alomari, M.A., Al-Farhany, K., Hashem, A.L., Al-Dawody, M.F., Redouane, F. and Olayemi, O.A. (2021) Numerical Study of MHD Natural Convection in Trapezoidal Enclosure Filled with (50%MgO-50%Ag/Water) Hybrid Nanofluid: Heated Sinusoidal from Below. *International Journal of Heat and Technology*, **39**, 1271-1279. https://doi.org/10.18280/ijht.390425

[27] Dogonchi, A.S., Sadeghi, M.S., Ghodrat, M., Chamkha, A.J., Elmasry, Y. and Alsulami, R. (2021) Natural Convection and Entropy Generation of a Nanoliquid in a Crown Wavy Cavity: Effect of Thermo-Physical Parameters and Cavity Shape. *Case Studies in Thermal Engineering*, **27**, Article 101208. https://doi.org/10.1016/j.csite.2021.101208

[28] Alsabery, A.I., Tayebi, T., Kadhim, H.T., Ghalambaz, M., Hashim, I. and Chamkha, A.J. (2021) Impact of Two-Phase Hybrid Nanofluid Approach on Mixed Convection Inside Wavy Lid-Driven Cavity Having Localized Solid Block. *Journal of Advanced Research*, **30**, 63-74. https://doi.org/10.1016/j.jare.2020.09.008

[29] Zeb Khan, N., Bilal, S., Riaz, A. and Muhammad, T. (2024) Coupled Effects of Variable Permeability and Adiabatic Undulating Walls on Natural Convective Flow in a Trapezoidal Cavity: Finite Element Analysis. *Results in Physics*, **56**, Article 107267. https://doi.org/10.1016/j.rinp.2023.107267

[30] Mohammed, A.A., Thaer, M. and Yahya, D.Q. (2022) Mixed Convection Heat Transfer of $Al_2O_3$-$H_2O$ Nanofluid in a Trapezoidal Lid-Driven Cavity at Different Angles of Inclination. *Texas Journal of Engineering and Technology*, **11**, 20-30.

[31] Uddin, M.N., Alim, M.A. and Bhuiyan, A.H. (2016) Effects of Circular Cylindrical Block on Heat Flow for MHD Free Convection in a Non-Uniformly Heated Trapezoidal Enclosure. *International Journal of Engineering & Applied Sciences*, **8**, 40-48. https://doi.org/10.24107/ijeas.255034

[32] Alnajem, M.H.S., Alsabery, A.I. and Hashim, I. (2019) Entropy Generation and Natural Convection in a Wavy-Wall Cavity Filled with a Nanofluid and Containing an Inner Solid Cylinder. *Proceedings of the* 2*nd International Conference on Sustainable Engineering Techniques* (*ICSET* 2019), *IOP Conference Series: Materials Science and Engineering*, **518**, Article 032044. https://doi.org/10.1088/1757-899x/518/3/032044

[33] Mejbel, A., Abdulkadhim, A., Hamzah, R., Hamzah, H. and Ali, F. (2020) Natural Convection Heat Transfer for Adiabatic Circular Cylinder Inside Trapezoidal Enclosure Filled with Nanofluid Superposed Porous-Nanofluid Layer. *FME Transactions*, **48**, 82-89.

[34] Ali, M.Y., Alim, M.A. and Karim, M.M. (2023) Mixed Convective Heat Transfer Analysis by Heatlines on a Lid-Driven Cavity Having Heated Wavy Wall Containing Tilted Square Obstacle. *Mathematical Problems in Engineering*, **2023**, Article ID: 1374926. https://doi.org/10.1155/2023/1374926

[35] Alesbe, I., Ibrahim, S.H. and Aljabair, S. (2021) Mixed Convection Heat Transfer in Multi-Lid-Driven Trapezoidal Annulus Filled with Hybrid Nanofluid. *Journal of Physics*: *Conference Series*, **1973**, Article 012065. https://doi.org/10.1088/1742-6596/1973/1/012065

[36] Akter, A. and Parvin, S. (2018) Analysis of Natural Convection Flow in a Trapezoidal Cavity Containing a Rectangular Heated Body in Presence of External Oriented Magnetic Field. *Journal of Scientific Research*, **10**, 11-23. https://doi.org/10.3329/jsr.v10i1.33848

[37] Ishak, M.S., Alsabery, A.I., Hashim, I. and Chamkha, A.J. (2021) Entropy Production and Mixed Convection within Trapezoidal Cavity Having Nanofluids and Localised Solid Cylinder. *Scientific Reports*, **11**, Article No. 14700. https://doi.org/10.1038/s41598-021-94238-w

[38] Chowdhury, K. and Alim, M.A. (2023) Mixed Convection in a Double Lid-Driven Wavy Shaped Cavity Filled with Nanofluid Subject to Magnetic Field and Internal Heat Source. *Journal of Applied Mathematics*, **2023**, Article ID: 7117186. https://doi.org/10.1155/2023/7117186

[39] Alsabery, A.I., Vaezi, M., Tayebi, T., Hashim, I., Ghalambaz, M. and Chamkha, A.J. (2022) Nanofluid Mixed Convection Inside Wavy Cavity with Heat Source: A Non-Homogeneous Study. *Case Studies in Thermal Engineering*, **34**, Article 102049. https://doi.org/10.1016/j.csite.2022.102049

[40] Alsabery, A.I., Ghalambaz, M., Armaghani, T., Chamkha, A., Hashim, I. and Saffari Pour, M. (2020) Role of Rotating Cylinder toward Mixed Convection Inside a Wavy Heated Cavity via Two-Phase Nanofluid Concept. *Nanomaterials*, **10**, Article 1138. https://doi.org/10.3390/nano10061138

[41] Ashorynejad, H.R. and Shahriari, A. (2018) MHD Natural Convection of Hybrid Nanofluid in an Open Wavy Cavity. *Results in Physics*, **9**, 440-455. https://doi.org/10.1016/j.rinp.2018.02.045

[42] Boulahia, Z., Wakif, A., Chamkha, A.J., Amanulla, C.H. and Sehaqui, R. (2019) Effects of Wavy Wall Amplitudes on Mixed Convection Heat Transfer in a Ventilated Wavy Cavity Filled by Copper-Water Nanofluid Containing a Central Circular Cold Body. *Journal of Nanofluids*, **8**, 1170-1178. https://doi.org/10.1166/jon.2019.1654

[43] Rabbi, K.M., Saha, S., Mojumder, S., Rahman, M.M., Saidur, R. and Ibrahim, T.A. (2016) Numerical Investigation of Pure Mixed Convection in a Ferrofluid-Filled Lid-Driven Cavity for Different Heater Configurations. *Alexandria Engineering Journal*, **55**, 127-139. https://doi.org/10.1016/j.aej.2015.12.021

[44] Toghraie, D. (2020) Numerical Simulation on MHD Mixed Convection of Cu-Water Nanofluid in a Trapezoidal Lid-Driven Cavity. *International Journal of Applied Electromagnetics and Mechanics*, **62**, 683-710. https://doi.org/10.3233/jae-190123

[45] Mahmud, M.J., Rais, A.I., Hossain, M.R. and Saha, S. (2022) Conjugate Mixed Convection Heat Transfer with Internal Heat Generation in a Lid-Driven Enclosure with Spinning Solid Cylinder. *Heliyon*, **8**, e11968. https://doi.org/10.1016/j.heliyon.2022.e11968